International Journal of the Physical Sciences Vol. 5(11), pp. 1757-1769, 18 September, 2010
Available online at http://www.academicjournals.org/IJPS
ISSN 1992 - 1950 ©2010 Academic Journals

Full Length Research Paper

Geophysical investigation in the Lower Benue trough of Nigeria using gravity method

Ugbor, D. O. and Okeke, F. N*

Department of Physics and Astronomy, University of Nigeria, Nsukka, Nigeria.

Accepted 06 September, 2010

Gravity survey in parts of Akataka and the environs in Abakaliki area of the Lower Benue trough was conducted over an area between longitudes 8°42′ E to 8°47′ E and latitudes 6°35′ N to 6°45 ′ N. Ninety eight gravity stations were occupied and the data collected were reduced relative to a base station. The geometry of the buried body was determined from the interpretation of residual anomaly data. Spherical model was assumed for the anomalous body based on the local geology and the residual gravity anomaly. A density contrast of 0.32 gcm^{-3} was calculated for the body. The residualized and interpreted gravity profiles yielded results that reveal low Bouguer gravity anomalies with magnitudes ranging from –2.5 to 3.8 mgals and with abrupt changes at intervals thereby suggesting a fault. The low-density anomalous body suspected to be salt deposit was buried at depths of between 868 and 2618 m. Its diameter ranging between 2,126 and 3,322 m, mass ranges from 1.18 to 4.52 × 10^{13} kg. The low Bouguer gravity anomaly over the area suggests a zone of basic to intermediate igneous intrusions, deep basement and crustal thinning. These calculated values are in agreement with other works carried out within Abakaliki areas in particular and the Lower Benue trough in general.

Key words: Gravity survey, profiles, Benue trough, intrusions, salt deposit, density.

INTRODUCTION

The Benue Trough is generally known to contain numerous mafic and felsic intrusives, sub-basinal structures together with a bright prospect for hydrocarbon accumulation. The aim of this present study is therefore, to carry out geophysical investigation in the lower section of the trough (Akataka and the environs in Ebonyi State) (Figure 1) using the gravity method. The depth to the suspected mineral body and the lateral extent are the most sought gravity parameters in this work. The objective of the work is to reveal as much as possible the geology and geophysical features of the area. Parameters like depth to suspected mineral deposits (salt) would be compared with depths of anomalies that were determined by other workers in areas close to where the present work is carried out. This work is however, guided by few works that have been carried out in Abakaliki areas as attempt is made to confirm or disagree with the earlier works by correlation.

The Benue Trough being generally regarded as a rift structure is noted to have many features in common with other intra-continental rifts. According to Shemang et al. (2005), the Benue rift can be compared with some well-known rift systems such as the East African, the Rhine Graben, the Baikal rift and the Rio Graande rift. These rift systems are all associated with volcanism and regional uplift. Mareschal (1983) indicated the basic geophysical characteristics of a rift as having a thin crust, a low velocity and density upper mantle and higher than normal heat flow. Many workers and researchers have focused a lot of attention on the trough. These are aimed at depicting the nature and characteristics of the structure. The earliest studies in the Benue Trough were mainly aimed at exploring its origin and tectonic evolution.

However, the earliest geophysical investigations in the Benue Trough were mainly centered on the measurement and rather qualitative study of its gravity field. The occurrence of lead-zinc mineralization, salt deposits and bright prospects of finding oil and uranium deposits in the trough have turned the area into one of great economic importance. The trough is a potential

*Corresponding author. E-mail: franciscaokeke@yahoo.com.

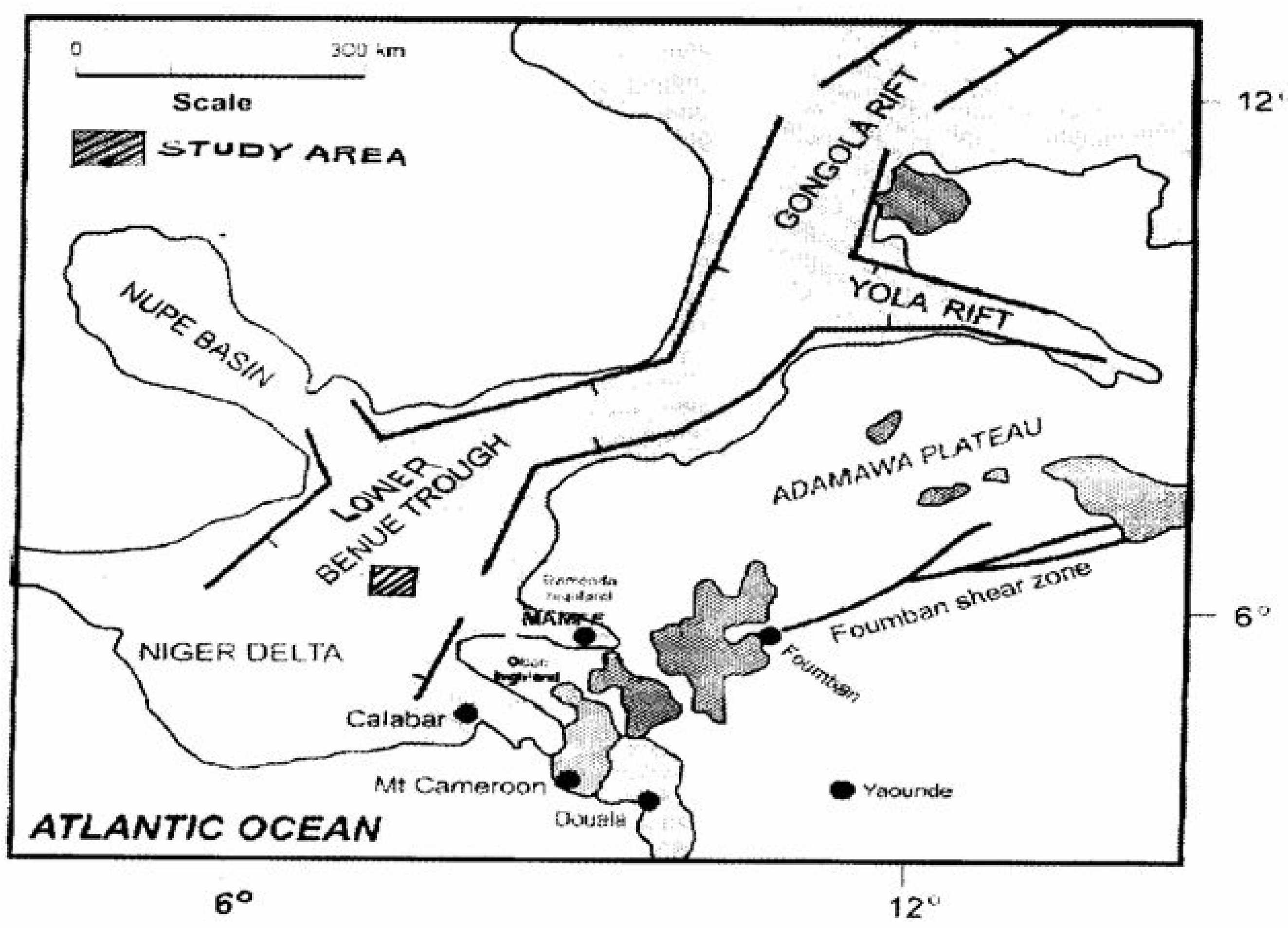

Figure 1. The Benue Trough with associated rifts with the study area indicated (Fairhead et al., 1987).

reservoir of enormous mineral resources. Obaje et al. (1999) claimed that the coal resources of Nigeria are located mainly within the Benne Trough, especially within the lower region.

There has been more extensive and intensive geological activites in the trough with renewed attempts at more detailed geophysical studies in the past few years. This has led not only to a better understanding of the structure of the Benue Trough, but also its origin and evolution. Nwachukwu (1972) studied it in terms of marine transgression and regression. Shemang et al. (2005) investigated the gravity anomalies over the Gongola Arm of the Upper Benne Trough. In their findings, they concluded that the results of the interpretation of gravity anomalies suggest the existence of intra basement intrusives of high densities in the trough at depths between about 0.5 and 2 km. The existence of intrusives suggests the existence of deeply penetrating fractures within the area. This conforms with basic intrusive which have been inferred from results of geophysical studies in different parts of the world over major rift systems such as the Rhine Graben and Baikal rift (Logatchev, 1993). Onyedim et al. (2009) interpreted the fault pattern in the basement within the middle Benue Trough by analyzing the topographic surface of the basement obtained by inverting gravity data. They were able to show that the major faults on the inversion surface for the band pass filtered data trend NE – SW and NW – SE. They also inferred that in places segments of these faults form bounding faults to sub – basins in the area. Ajakaiye (1981) suggested that the Bouguer anomalies observed in the trough ranges in value from 60 to 400 g.u., and that the free air anomaly values are close to zero except for the local attainment of values of 300g.u. Cratchley and Jones (1965) carried out an extensive gravity survey of the Benue Trough and concluded that the whole area was isostatically compensated. Ajayi (1991) suggests that the magnitudes of the gravity anomalies locally associated with the prominent salt springs in Nigeria's Middle Benue range from -1.1 to -5.7 mgals. The preliminary interpretations of these anomalies suggest the possible existence of small to medium sized salt domes buried at moderate to intermediate depths of 0.5 to 1.8 km. On the other hand, Nkwonta and Kene (2005) employed various graphical methods of aeromagnetic interpretation to determine the depth to the buried magnetic anomalous structures in the Lower Benue trough. They discovered that the depth to the top of the structure lies between 0.55 and 9.20 km. They inferred that the magnetic anomalies over parts of the trough could be explained by the existence of the intrusive bodies and elevation of crystalline basement.

METHODOLOGY

Gravity survey method was employed in this work. The present work was carried out on land in Akataka and the environs using the worden gravimeter. In selecting the location, we considered accessibility to the gravity stations and laid out our gravimeter stations along existing tracks and major road networks at intervals of 500 m except in some cases where the distances were less, due to lack of access paths and sometimes due to lack of water transport.

The fieldwork was carried out between the months of November and January. This period of the year was selected to prevent disruption of smooth field operations by intermittent rainfalls that characterize the location between April and October. During the period of data acquisition, we first established a base station from where the gravity differences along the other stations were measured. The base was re-visited at every 2 h and readings repeated which helped in accounting for the instrument drift. At each station, the actual time of setting up and reading the instrument was only a few (1 to 15 min) minutes.

In obtaining a set of readings for a gravity station, the gravimeter base plate was first leveled and the scale reading of the gravimeter taken. The elevations of the gravimeter stations were determined by an altimeter and the geographical location of the station determined by compass. These parameters were applied in reducing the readings to standard reference conditions before the data analysis. Bouguer gravity anomalies resulting from the corrected gravity data were contoured. Seven profiles running across contour closures were considered. The observed gravity anomalies along the profiles were separated into regional and residual gravity anomalies, employing a graphical method of residualising. Some rock samples exposed in the survey areas were also collected during the fieldwork. These rock samples were later analyzed in the laboratory and their average density obtained. It was then discovered that the average density of rocks surrounding the formations are appreciably different from those of the formation itself, resulting in the density contrast employed in the interpretation.

Reduction of gravity data from field work

Table 1 shows a sample of the gravity field readings and reductions on 23rd January for 98 gravity stations used in this work. The readings of the first seven columns are raw field readings from which values in the other columns are calculated.

Bouguer gravity anomaly contour map

After obtaining column 15 in Table 1 for the stations, the positions of the stations are mapped with their corresponding Bouguer gravity anomaly values. Matlab program was then used in ploting these Bouguer anomaly values on an appropriate map. By using the Matlab program command, smooth curves (iso- anomaly) are drawn to connect points with equal anomaly.

Gravity profiles

These are straight lines drawn to cut across the contour lines on the Bouguer anomaly map. The profiles intersect with the contour lines at values, which indicate the variation of Bouguer anomaly with horizontal distance in the survey area. For the purpose of the present study, seven profiles are considered. These are named accordingly as AA′, BB′, CC′, DD′, EE′, FF’ and GG’ as shown in Figure 2. We choose profiles that run across closures of contours where the effects of the anomaly were highest.

Profiles AA′, CC′, DD′, and EE′ run from N – W to S – E while profile BB′ run from S – W to N – E. Stations FF′ and GG′ run N – S, all aimed at crossing some degrees of closures. Along each of these profiles, we were able to determine the corresponding observed gravity anomaly along the horizontal distance. The regional trend was chosen to match with the sign of our density contrast, which then aided the determination of the residual gravity anomaly along the same horizontal distance. These values were then used in plotting Bouguer gravity anomaly and residual gravity anomaly against horizontal distances.

The variations of the observed Bouguer gravity anomalies with the horizontal distance along profile AA′ to GG′ are shown in Figures 3a, 4a, 5a, 6a, 7a, 8a and 9a. Smooth regional trends were estimated and drawn in the figures using the same axes. In the present work, the density contrast was negative with value of – 0.32gcm^{-3}.

The residual gravity anomaly was then obtained as the difference between the two curves (that is, observed gravity anomaly – regional trend). It contains the components of the field, which presumably are caused by mass irregularities representing geologic disturbances of interest. It was also plotted against the horizontal distance as shown in Figures 3b, 4b, 5b, 6b, 7b, 8b and 9b for profiles AA′ to GG′ respectively. These local disturbances in gravity along the study areas were used in calculating the characteristics of the intrusive body giving the anomaly.

Interpretation of the profiles

The residual Bouguer gravity anomalies along the profiles suggest the presence of anomalous body within the zone. The geology of the area suggests a spherical body and hence, the sphere model is employed to estimate the sought parameters of the anomaly. These include: depth from surface to centre z, radius R, depth to surface T and the mass of the body, M.
Thus, to find the depth to center we employ the following equations;

$$g_z = \frac{4\Pi G R^3 \rho}{3z^2} \frac{1}{\left(1+\frac{x^2}{z^2}\right)^{3/2}} = g_o \frac{1}{\left(1+\frac{x^2}{z^2}\right)^{3/2}} \quad \text{(Telford et al., 1990)} \qquad (1)$$

At half width $x_{1/2}$,

$$\left[\frac{1}{1+\left(\frac{x}{z}\right)^2}\right]^{3/2} = \frac{1}{2}$$

Table 1. Gravity field reading for 23rd January, 2006.

Station	Elevation (M)	Base plate height (M)	Time (GMT)	Gravimeter reading (scale division)	Latitude (N 6°)	Longitude (E 8°)	Drift correction (scale division)	Reading corrected for drift (scale division)	Drift corrected gravity difference relative to base station A_1 (MGALS)	Free- air correction relative to A_1 (MGALS)	Bouguer plate correction relative to A_1 (MGALS)	Combined elevation correction (MGALS)	Latitude correction (MGALS)	Bouguer anomaly (MGALS)
A_1	81.68	0.053	12:15	1759.50	37.63′	42.02′	0.00	1759.50	0.000	0.000	0.000	0.000	0.000	0.000
A_2	72.84	0.050	13:08	1760.65	37.66′	42.02′	-0.86	1759.79	0.030	-2.728	-0.990	-1.738	0.010	-1.698
A_3	81.07	0.060	13:21	1761.10	37.69′	42.02′	-1.20	1759.90	0.042	-0.188	-0.068	-0.120	0.021	-0.057
A_4	82.84	0.064	13:30	1760.98	37.71′	42.02′	-1.04	1759.94	0.046	-0.358	0.130	0.228	0.026	0.300
A_5	74.90	0.055	13:43	1761.30	37.74′	42.12′	-1.28	1760.02	0.054	-2.092	-0.759	-1.333	0.037	-1.242
A_6	85.64	0.056	13:56	1760.79	37.77′	42.02′	-0.68	1760.11	0.063	1.222	0.443	0.779	0.047	0.889
A_7	85.34	0.053	14:11	1760.51	37.92′	42.28′	-0.32	1760.19	0.072	1.129	0.410	0.719	0.100	0.891
A_8	87.17	0.049	14:28	1760.72	38.06′	42.61′	-0.44	1760.28	0.081	1.694	0.615	1.079	0.146	1.306
A_9	86.56	0.048	14:42	1760.15	38.12′	42.90′	0.24	1760.39	0.092	1.506	0.546	0.960	0.167	1.219
A_{10}	89.91	0.051	14:54	1760.39	38.55′	43.10′	0.08	1760.47	0.101	2.540	0.921	1.619	0.317	2.037
B_2	90.83	0.064	15:29	1760.32	37.81′	42.09′	0.08	1760.04	0.056	2.824	1.064	1.760	0.062	1.878
B_3	89.00	0.063	15:40	1760.80	38.93′	43.28′	-0.46	1760.34	0.088	2.259	0.819	1.440	0.219	1.747
B_4	88.39	0.062	15:52	1761.20	38.90′	43.25′	-0.93	1760.27	0.080	2.071	0.751	1.320	0.209	1.609
B_5	82.90	0.062	16:03	1761.40	40.20′	43.73′	-1.22	1760.18	0.071	0.376	0.137	0.239	0.658	0.968
B_6	83.21	0.055	16:14	1761.10	40.67′	43.99′	-0.96	1760.14	0.066	0.472	0.171	0.301	0.819	1.186
B_7	84.42	0.060	16:21	1760.92	40.58′	43.81′	-0.84	1760.08	0.060	0.846	0.307	0.539	0.788	1.387
B_8	80.16	0.060	16:34	1760.70	41.09′	43.88′	-0.70	1760.00	0.052	-0.469	-0.170	-0.299	0.965	0.718
B_9	77.72	0.064	16:44	1760.70	41.22′	43.03′	-0.78	1759.92	0.044	-1.222	-0.443	-0.779	1.011	0.276
B_{10}	77.11	0.060	16:57	1760.80	42.10′	44.33′	-0.96	1759.84	0.035	-1.410	-0.512	-0.898	1.317	0.454
B_{11}	80.46	0.056	17:09	1760.53	42.36′	44.82′	-0.76	1759.77	0.028	-0.376	-0.137	-0.239	1.407	1.196
B_{12}	78.63	0.062	17:18	1760.30	42.50′	44.76′	-0.61	1759.69	0.020	-0.941	-0.341	-0.600	1.454	1.474
B_{13}	79.55	0.050	17:30	1760.48	42.27′	45.16′	-0.86	1759.62	0.013	-0.657	-0.238	-0.419	1.375	0.969
B_{14}	79.24	0.057	17:42	1760.32	41.21′	44.80′	-0.80	1759.52	0.002	-0.753	-0.273	-0.480	1.006	0.528
B_{15}	80.77	0.060	17:51	1760.40	42.11′	44.01′	-0.92	1759.48	0.002	-0.281	-0.102	-0.179	1.319	1.142
B_{16}	81.07	0.063	18:03	1760.58	42.50′	45.67′	-1.18	1759.40	0.010	-0.188	-0.068	-0.120	1.803	1.693

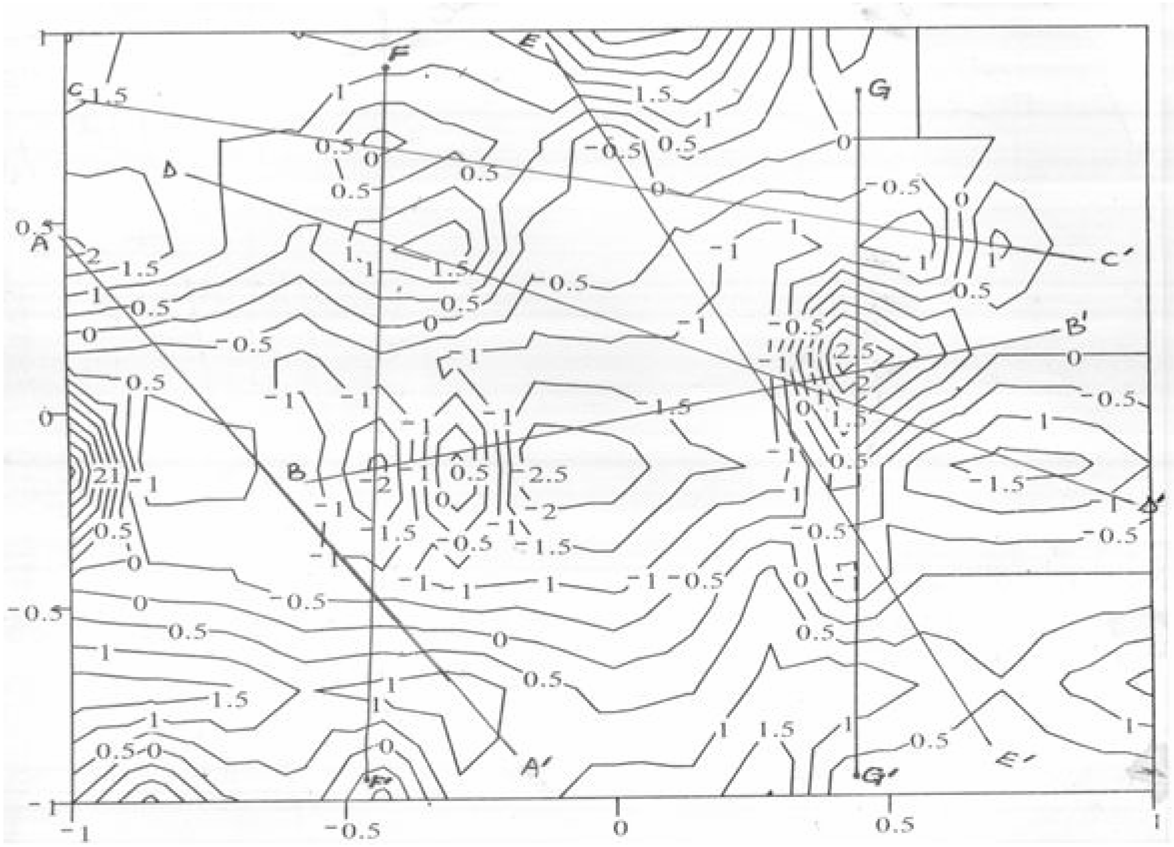

Figure 2. Bouguer gravity anomaly contour map.

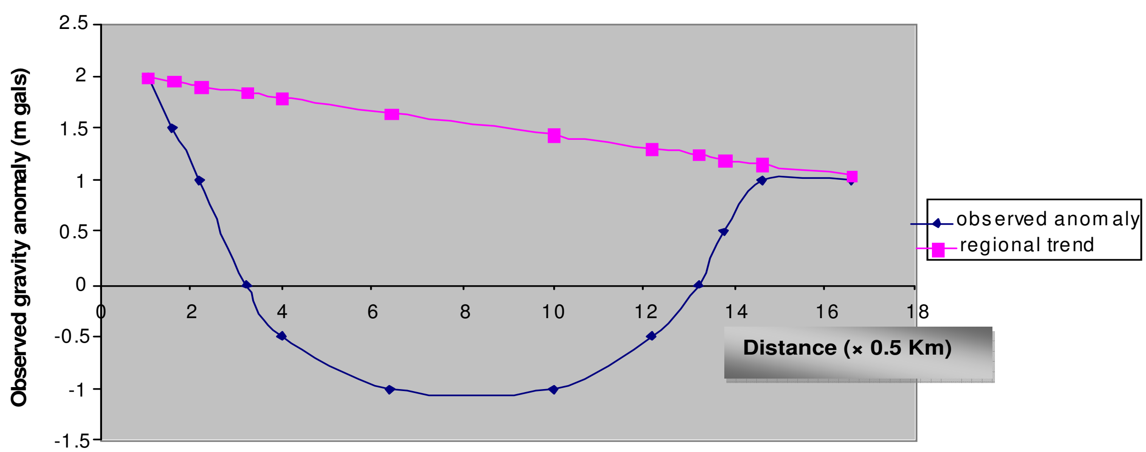

Figure 3a. Observed Bouguer gravity anomaly along AA′ and the estimated regional trend (Profile AA’).

Solving the above equation gives $z = 1.305 x_{1/2}$ (2)

Gravity profile Aa'

From Figure 3b: i) Half width, $x_{1/2}$ = 2.4km = 2400m

⇒Depth from surface to centre of anomaly, z = 1.305 x 2400 = 3132.0 m;

ii) Radius of anomaly can be obtained by employing equation:

$$R = \left(\frac{3 z^2 \Delta g_o}{4 \Pi G \rho} \right)^{1/3}$$ (Telford et al., 19900) (3)

A **A′**

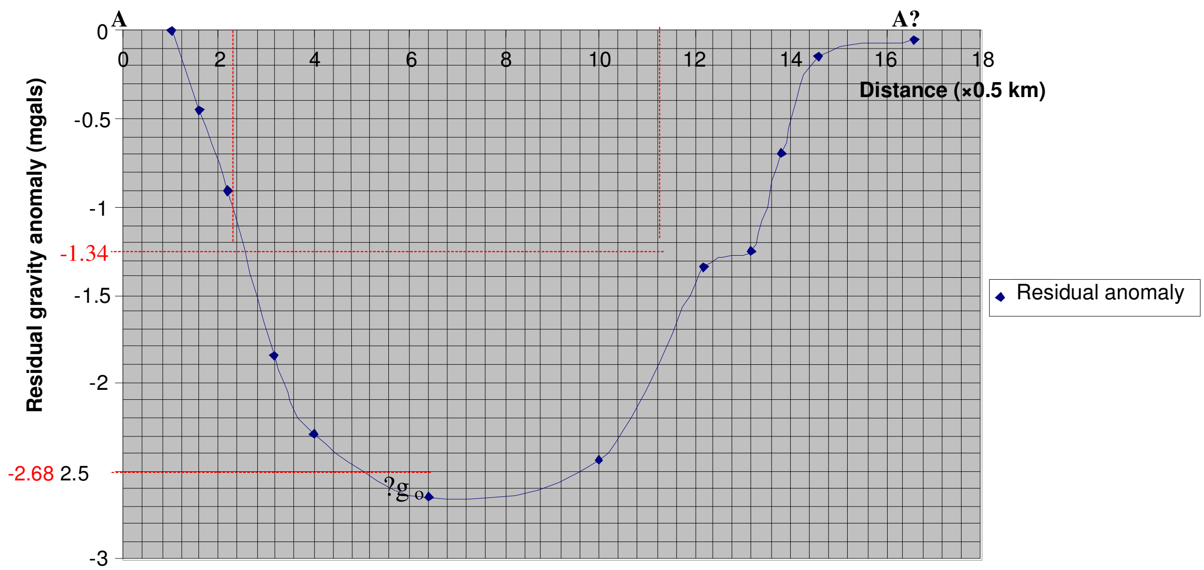

Figure 3(b). Residual bouguer gravity anomaly along AA′.

where, $\rho = \rho_a - \rho_c$ and ρ_a is the average density of rock salt collected from the study area which is approximately 2.35 gcm^{-3} while ρ_c is the mean density of surrounding crustal rock taken as 2.67 gcm^{-3}.

Hence, density contrast $\rho = (2.35 - 2.67)\ gcm^{-3} = -0.32 gcm^{-3}$ or 320 kgm^{-3}.

Thus, $R = \left[\frac{3(3132)^2 \times 2.68 \times 10^{-5}}{4\pi \times 6.67 \times 10^{-11} \times 320}\right]^{1/3}$ = 1432.64 m.

iii) Depth to surface of anomaly using equations 2 and 3 give
T = Z – R = 3132.00 - 1432.64 = 1699.36 M.

iv) Mass of anomaly, M = density x volume

$$M = \frac{4\Pi R^3 \rho_a}{3} \quad \text{(Telford et al., 19900)} \qquad (4)$$

$$= \frac{4\pi \times (1432.64)^3 \times 2350}{3}$$

= 2.8945×10^{13}kg.

Gravity profile BB'

From Figure 4b,

Half width, $x_{1/2}$ = 1.48 km = 1480 m

z = 1.305 × 1480
= 1931.40 m

ii) Radius of anomaly, $R = \left[\frac{3(1931.40)^2 \times 2.88 \times 10^{-5}}{4\pi \times 6.67 \times 10^{-11} \times 320}\right]^{1/3}$

= 1063.14 m

iii) Depth to surface, T = 1931.40 – 1063.14 = 868.26 m

iv) Mass of anomaly,

$$M = \frac{4\pi(1063.14)^3 \times 2350}{3}$$

= 1.1828×10^{13}kg

Gravity profile cc'

From Figure 5b

i) Half width, $x_{1/2}$ =1.9km = 1900m

z = 1.305 × 1900 = 2479.50 m

ii) Radius of anomaly:

$$R = \left[\frac{3(2479.50)^2 \times 2.12 \times 10^{-5}}{4\pi \times 6.67 \times 10^{-11} \times 320}\right]^{1/3}$$ = 1133.88 m

iii) Depth to surface, T = 2479.50- 1133.88 = 1345.62 m

iv) Mass of anomaly:

$$M = \frac{4\pi(1133.88)^3 \times 2350}{3}$$

= 1.4350×10^{13}kg

Gravity profile DD'

From Figure 6b

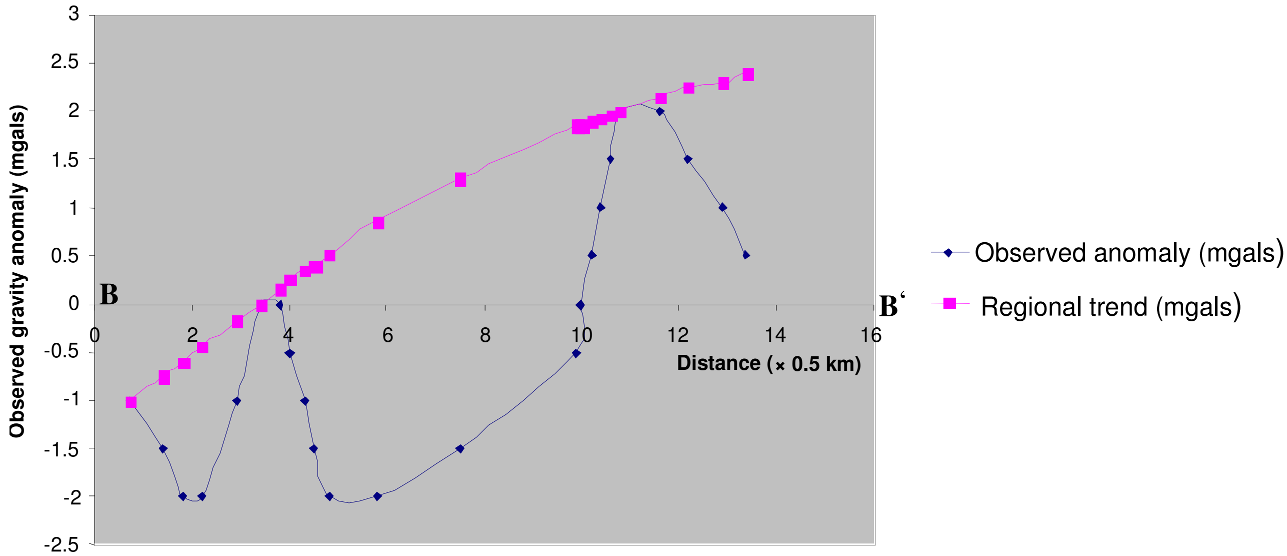

Figure 4(a). Observed Bouguer gravity anomaly along BB′ and the estimated regional trend (Profile BB’).

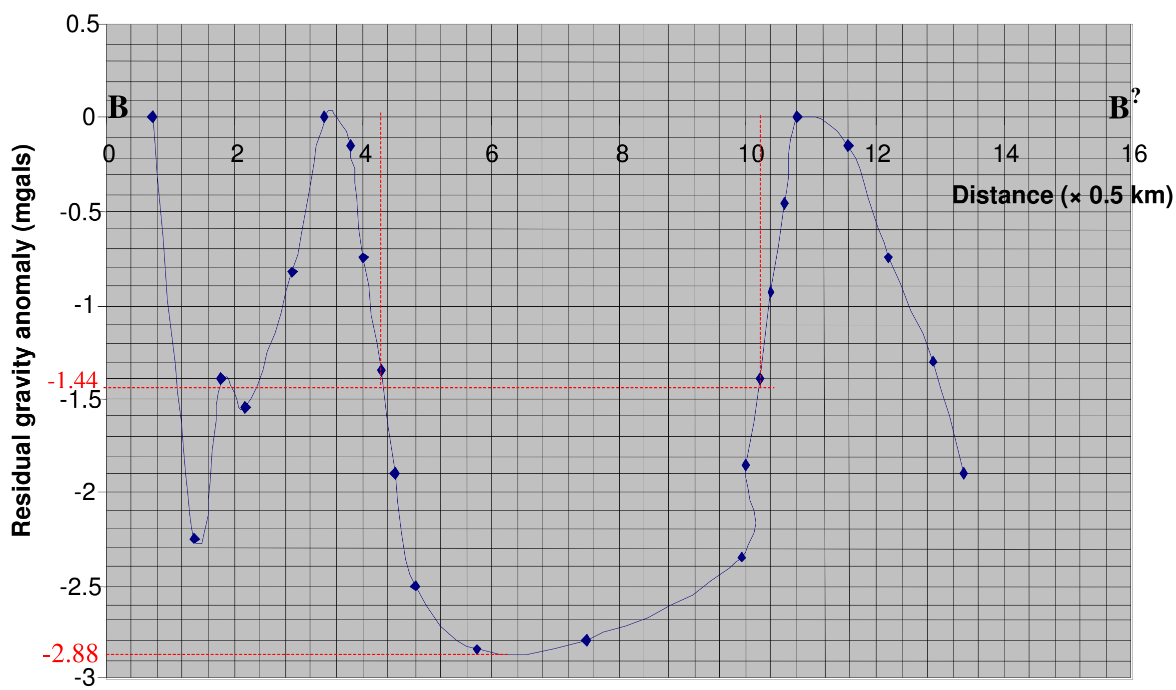

Figure 4(b). Residual Bouguer gravity anomaly along BB′.

i) Half width, $x_{1/2}$ =1.58 km = 1580 m

z = 1.305 × 1580
= 2061.90 m

ii) Radius of anomaly:

$$R = \left[\frac{3(2061.90)^2 \times 2.80 \times 10^{-5}}{4\pi \times 6.67 \times 10^{-11} \times 320} \right]^{1/3} = 1100.13\text{m}$$

iii) Depth to surface, T = 2061.90-1100.13
= 961.77 m

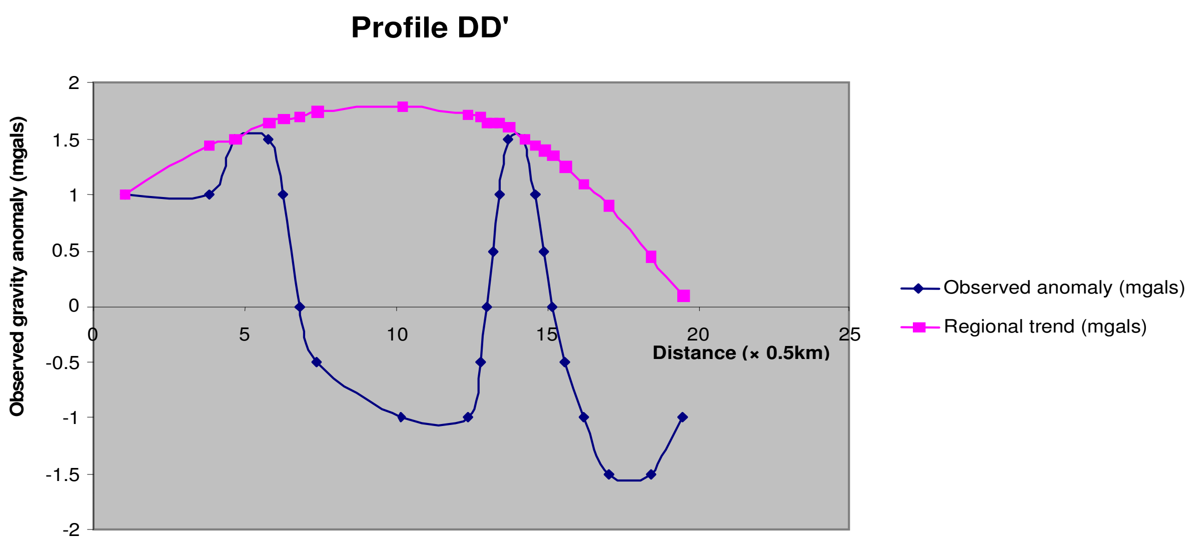

Figure 5a. Observed Bouguer gravity anomaly along CC′ and the estimated regional trend.

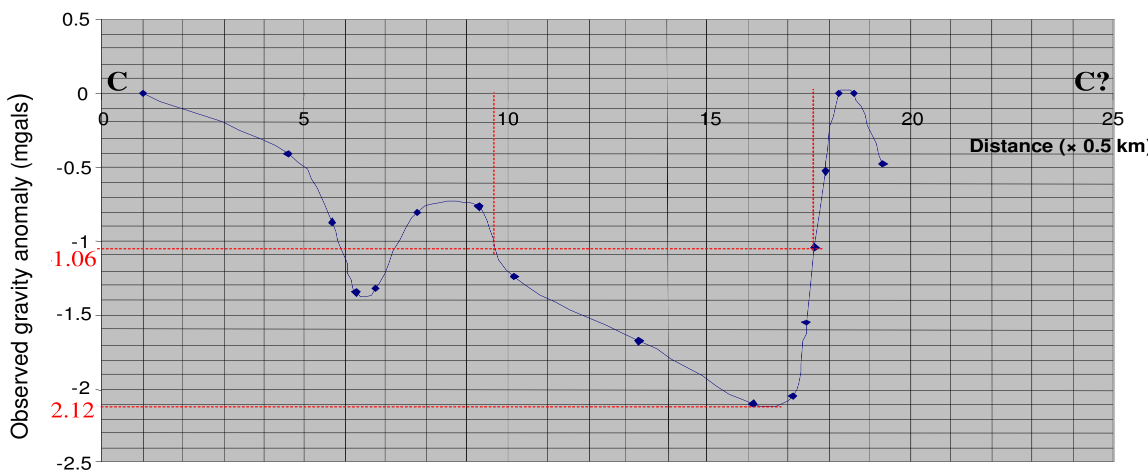

Figure 5b. Residual Bouguer gravity anomaly along CC′.

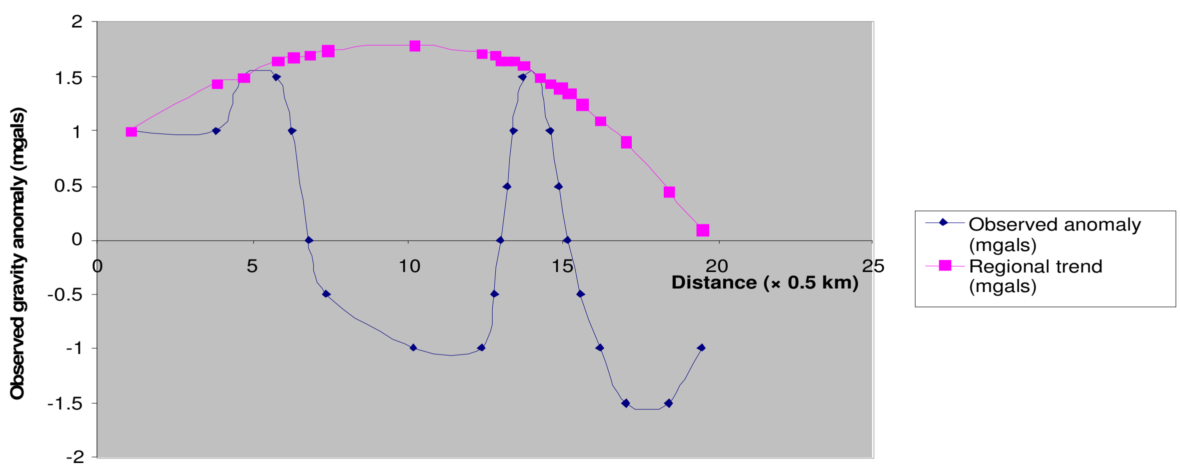

Figure 6a. Observed Bouguer gravity anomaly along DD′ and the estimated regional trend.

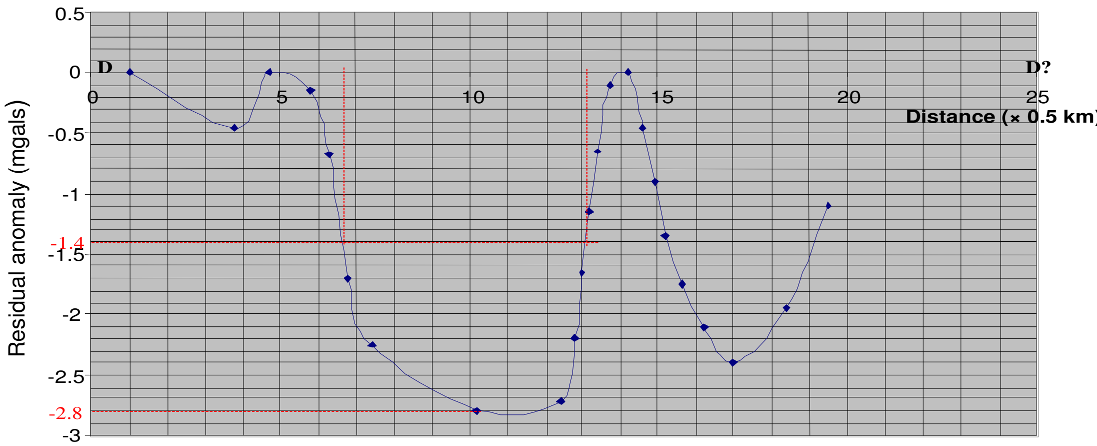

Figure 6b. Residual Bouguer gravity anomaly along DD′.

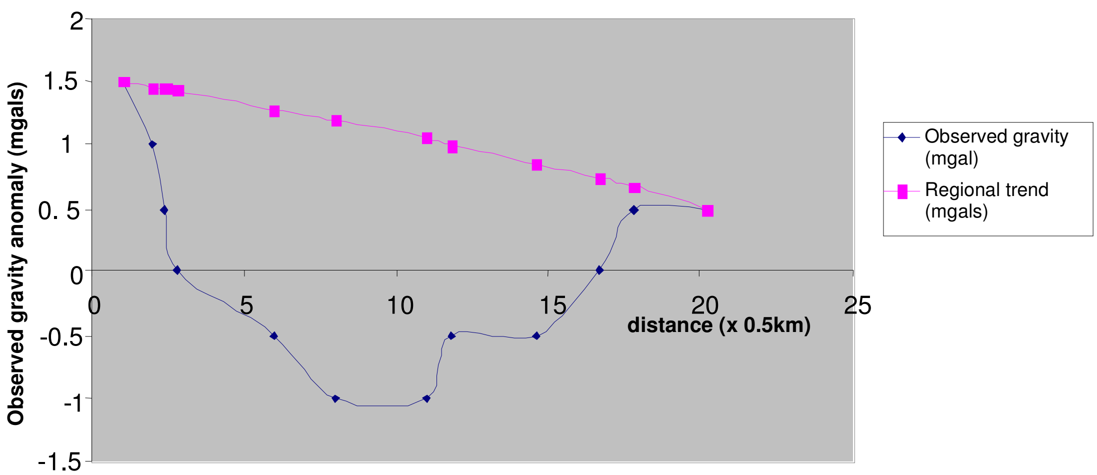

Figure 7a. Observed Bouguer gravity anomaly along EE′ and the estimated regional trend.

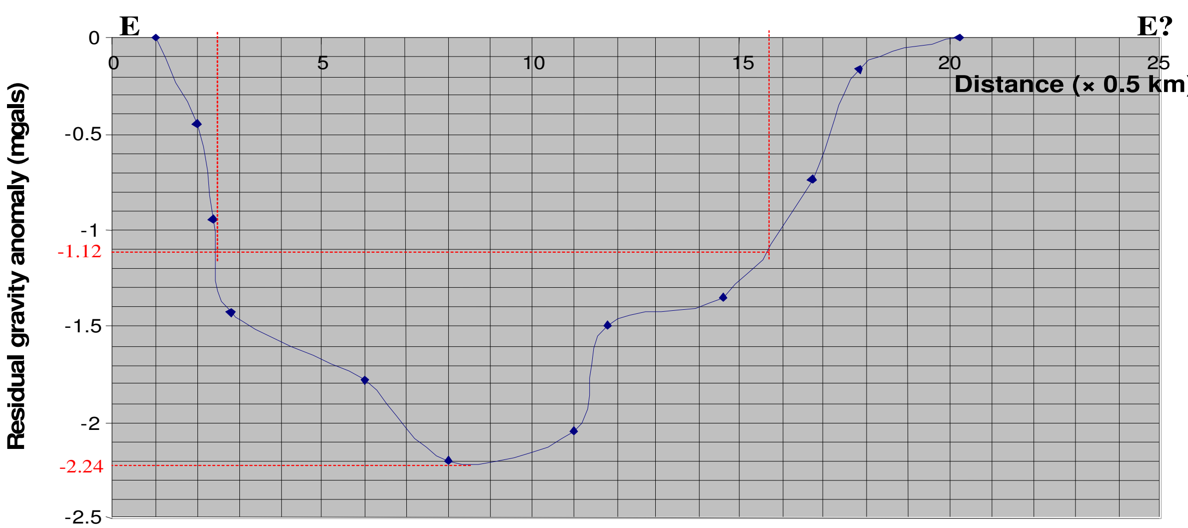

Figure 7b. Residual Bouguer gravity anomaly along EE′.

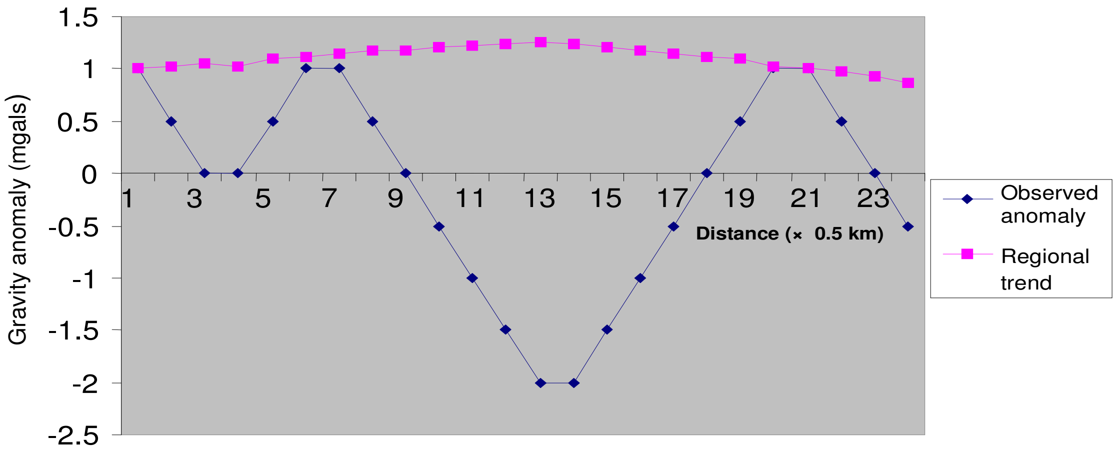

Figure 8a. Observed Bouguer gravity anomaly along FF′ and the estimated regional trend.

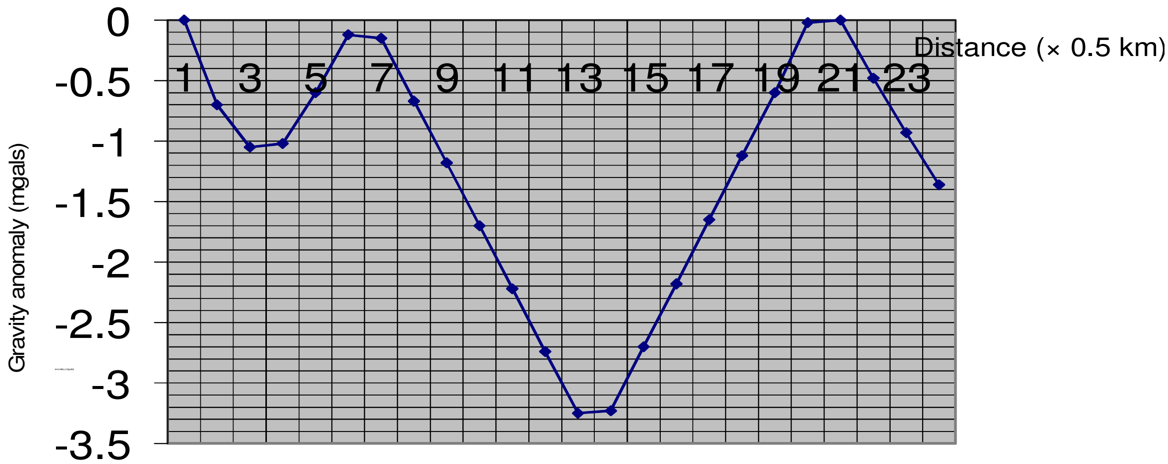

Figure 8b. Residual Bouguer gravity anomaly along FF′.

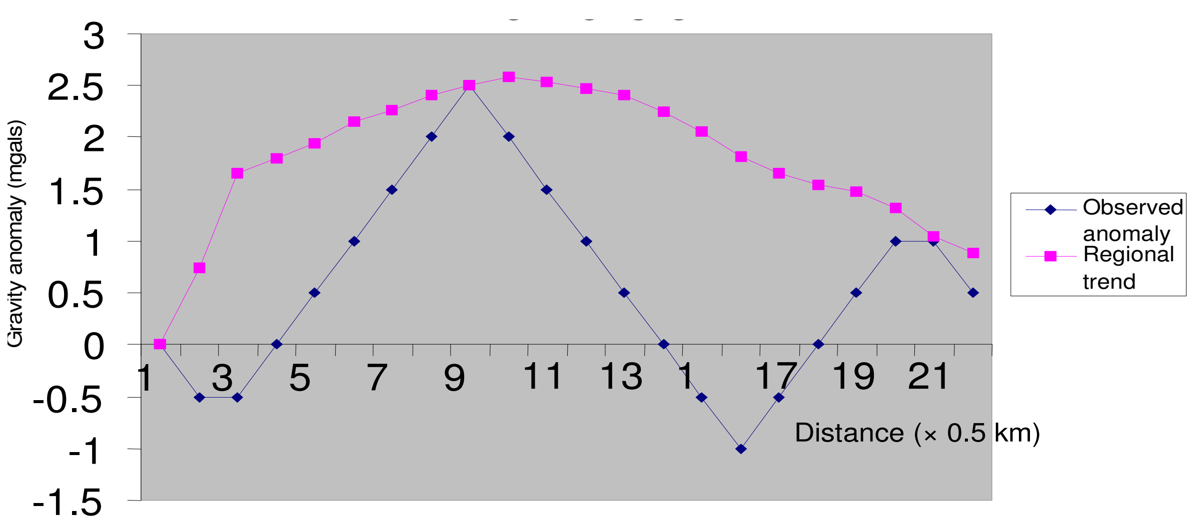

Figure 9a. Observed Bouguer gravity anomaly along GG′ and the estimated regional trend.

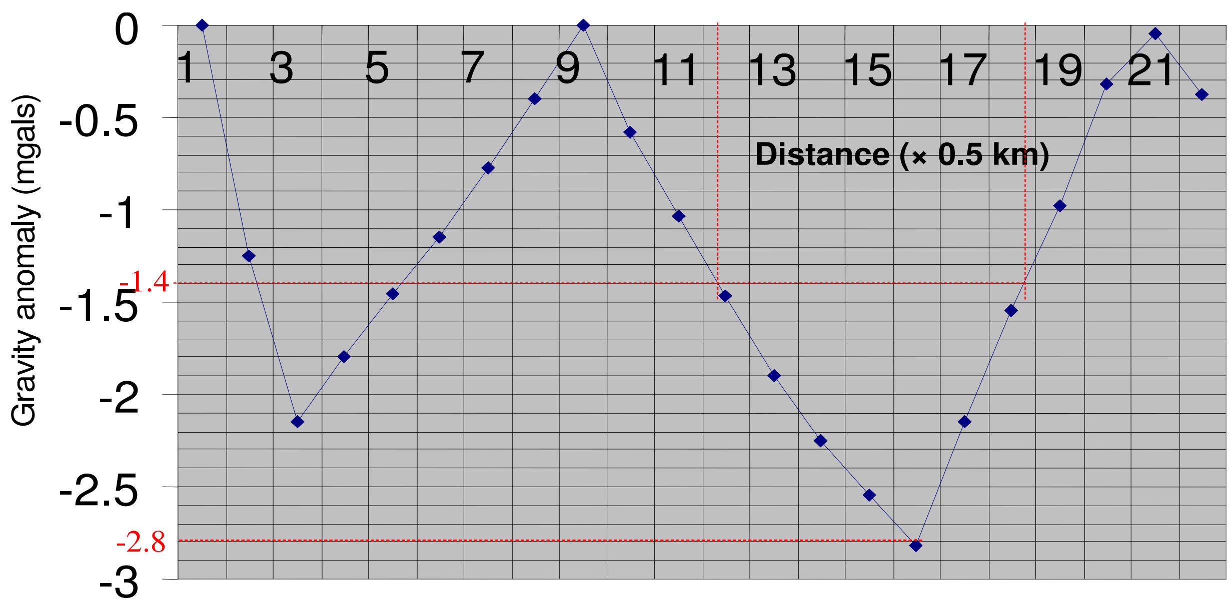

Figure 9b. Residual Bouguer gravity anomaly along GG′.

iv) Mass of anomaly, $M = \dfrac{4\pi(110013)^3 \times 2350}{3}$ = 1.3107 × 10^{13} kg

Gravity profile EE'

From Figure 7b:

i) Half width, $x_{1/2}$ =3.28km = 3280m

z = 1.305x3280
= 4280.40m

ii) Radius of anomaly:

$$R = \left[\frac{3(4280.40)^2 \times 2.24 \times 10^{-5}}{4\pi \times 6.67 \times 10^{-11} \times 320}\right]^{1/3}$$ = 1661.95m

iii) Depth to surface, T = 4280.40 - 1661.95
= 2618.45 m

Mass of anomaly, $M = \dfrac{4\pi(1661.95)^3 \times 2350}{3}$

= 4.5187 x 10^{13} kg

Gravity profile FF'

From Figure 8b,

Half width, $x_{1/2}$ = 1.75 km = 1750 m

z = 1.305 × 1750
= 2283.75 m

ii) Radius of anomaly:

$$R = \left[\frac{3(2283.75)^2 \times 2.88x10^{-5}}{4\pi \times 6.67x10^{-11} \times 320}\right]^{1/3}$$ = 1188.80m

iii) Depth to surface, T = 2283.75 – 1188.80
= 1094.95m

iv) Mass of anomaly,

$$M = \frac{4\pi(1188.80)^3 \times 2350}{3}$$ = 1.6538 x 10^{13}kg

Gravity profile GG'

From Figure 9b,

Half width, $x_{1/2}$ = 1.375 km = 1375 m

z = 1.305 × 1375
= 1794.38 m

ii) Radius of anomaly,

$$R = \left[\frac{3(179438)^2 \times 2.88 \times 10^{-5}}{4\pi \times 6.67 \times 10^{-11} \times 320}\right]^{1/3}$$ = 1012.24 m

iii) Depth to surface, T = 1794.38 – 1012.24
= 782.14 m

Table 2. Results of the interpretation.

Profile	Z(m)	R(m)	T(m)	M(kg)
AA′	3132.00	1432.64	1699.36	2.8945×10^{13}
BB′	1931.40	1063.14	868.26	1.1828×10^{13}
CC′	2479.50	1133.88	1345.64	1.4350×10^{13}
DD′	2061.90	1100.13	961.77	1.3107×10^{13}
EE′	4280.40	1661.95	2618.45	4.5187×10^{13}
FF′	2283.75	1188.80	1094.95	1.6538×10^{13}
GG′	1794.38	1012.24	782.14	1.021×10^{13}

iv) Mass of anomaly:

$$M = \frac{4\pi(1012.24)^3 \times 2350}{3} = 1.0210 \times 10^{13}\text{kg}$$

DISCUSSION

The gravity data from parts of Akataka area and environs has been reduced, analyzed and interpreted. The reduced data was critically analyzed using graphical method. Some parameters of the anomalous body were estimated along the seven gravity profiles analyzed on the Bouguer gravity contour map. Graphical residualising was employed in the analysis and based on known local geology and the nature of the residual Bouguer gravity anomalies a spherical model was assumed for body beneath the survey area. The depth, Z to the top surface from center, radius of the body R, depth to surface, T and mass, M of anomaly are summarized in Table 2.

From the results of the study, one can closely observe the correlation between profiles BB′, DD′ and GG′ with respect to the parameters calculated. It is important to note that these profiles pass through the areas where the contours closures are greatest (see figure 2). In other words, the closer the contours, the shallower or more superficial is the body responsible for the gravity effect felt on the surface. Profiles BB′ and DD′ pass through greatest closures with the anomaly manifesting through calculations to be situated at shallower depths. Profiles AA′ and EE′ passed through the least close contours with the anomalies deeply situated. It is interesting to have observed gravity lows which cause could be attributed to a large and massive anomalous low-density material whose depths of intrusion from surface to top range from 782 to 2618 m with radii and masses ranging from 1. 012 to 1,661 m and 1.02×10^{13} to 4.52×10^{13} kg, respectively. This suggests a zone of basic to intermediate igneous intrusions, deep basement and crustal thinning. Based on known local geology, low Bouguer gravity anomalies (with magnitudes ranging from –2.5 to 3.8 mgals and whose values changes abruptly from negative to positive as one moves from one station to another) and the calculated density of 2.35 gcm-^{3}, the area is suspected to hold rock salt deposit within these depths. These values are in agreement with other works carried out within the Abakaliki area as earlier reviewed in the literature.

Conclusion

Gravity field investigation was carried out in Akataka and the environs in Ebonyi state. Results from our analyses have helped in ascertaining the depth to the suspected mineral body and the lateral extent of this body. Furthermore, the geologic and geophysical features of the area were revealed. The low-density sub-surface body which invariably indicate presence of salt dome, buried at a depth between 868 and 2618 m implies presence of oil or/and Uranium in the area understudy. Consequently, Lower Benue trough still has attributes that make it an area for active research work.

RECOMMENDATIONS

A more detailed gravity survey to ensure uniform coverage in the entire Lower Benue trough, particularly in the Abakaliki areas be carried out. This will bring to bare the location, nature and depth of structures buried in the entire area. This will involve both the government, the private sectors, exploration companies and individuals committing money and resources. Apart from graphical method of calculating residuals, other analytical smoothing methods (such as empirical gridding, polynomial fitting, upward and downward continuation) should be employed. On the alternative, computer based interpretational procedures could also be applied. Future gravity works should be carried out in the area employing improved techniques.

REFERENCES

Ajakaiye DE (1981). Geophysical Investigation of the Benue trough – A Review. Earth Evol. Sci., 1: 126-136.

Ajayi CO (1991). Preliminary Interpretation of the Gravity Anomalies Associated with some Prominent Salt Springs in the Middle Benue Nigeria. J. Mining Geol., 27(1): 87- 94.

Cratchley CR, Jones GP (1965). An interpretation of geology and gravity anomalies of the Benue valley, Nigeria Geophys. Pap. Overseas Geol. Surv. London, No 1.
Fairhead JD, Okereke CS (1987). A Regional Gravity Study of the West African Rift System in Nigeria and Cameroun and its Tectonic Implication. Tectonophysics, 143: 141-159.
Logatcher NA (1993). History of Geodynamics of Baikal rift (East Siberia): A review. Bulletin due center de la recherché exploration production Elf Aquitanne, 17: 353 - 370.
Mareschal J (1983). Mechanisms of Uplift Preceeding Rifting. Tectonophysics, 94: 51-66.
Nkwonta IK, Kene PO (2005). Use of Aeromagnetics in Mineral / Structural Exploration in Nigeria. American Geophysical Union, Spring Meeting 2005, abstract #NS238 - 12.
Nwachukwu SO (1972). The Tectonic Evolution of the Southern Portion of the Benue Trough, Nigeria. Geol. Mag., 109: 411-419.
Obaje NG, Funtua II, Ligouis B, Abaa SI (1999). Organic Maturation and Coal- Derived Hydrocarbon Potentials of Cretaceous Coal Measures in the Middle Benue Trough of Nigeria. J. Mining and Geol., 34(1): 7-18.
Onyedim GC, Alagoa KD, Adedekun IO, Aderogba AA, Ovuru C (2009). Mapping high – angle basement faults in the Middle Benue Trough, Nigeria from Gravity Inversion Surface. Earth Sci. Res. J. (online), 2009, 13(2): 140-147.
Shemang EM, Jacoby WR, Ajayi CO (2005). Global J. Geological sci., 3(1): 61-69.
Telford WM, Geldart LP, Sheriff RE (1990). Applied Geophysics. Cambridge University Press, London.